

Inclusive (\vec{p}, α) reaction on ^{59}Co at an incident energy of 100 MeV and comparison with the reaction mechanism for ^{93}Nb between 65 and 160 MeV

A. A. Cowley,^{1,2,*} S. S. Dimitrova,^{3,4,†} E. V. Zemlyanaya,⁴ K. V. Lukyanov,⁴ and J. J. van Zyl¹

¹Department of Physics, Stellenbosch University, Private Bag X1, Matieland 7602, South Africa

²iThemba Laboratory for Accelerator Based Sciences, PO Box 722, Somerset West 7129, South Africa

³Institute for Nuclear Research and Nuclear Energy, Bulgarian Academy of Sciences, 1784 Sofia, Bulgaria

⁴Joint Institute for Nuclear Research, 141980 Dubna, Russia

(Received 16 November 2015; revised manuscript received 22 January 2016; published 31 March 2016)

Experimental results are presented for the inclusive reaction $^{59}\text{Co}(\vec{p}, \alpha)$ at an incident energy of 100 MeV. A theoretical analysis based on a statistical multistep mechanism indicates that the terminal step leading to emission of an α particle can be a pickup or knockout process and that both processes are very prominent. This is a conclusion which is in agreement with an earlier study of the $^{93}\text{Nb}(\vec{p}, \alpha)$ reaction. This inspires an investigation of the reason why a mixture of knockout and pickup is present at an incident energy of 100 MeV, whereas at both higher and lower incident energies knockout appears to dominate for the target nucleus ^{93}Nb . It is found that the different dynamics of the two competing reaction mechanisms provide an explanation for the observed phenomenon. It is speculated that for ^{59}Co at both lower and higher incident energies the trend is likely to be similar to that of ^{93}Nb .

DOI: [10.1103/PhysRevC.93.034624](https://doi.org/10.1103/PhysRevC.93.034624)

I. INTRODUCTION

The mechanism of proton-induced composite particle emission in inclusive reactions, such as $(\vec{p}, {}^3\text{He})$ and (\vec{p}, α) , at incident energies in the range from 65 to 200 MeV [1–5] is clearly linked to a multistep statistical process [6–8], which also drives pre-equilibrium nucleon emission. The multistep character of the reaction chain is especially prominently displayed in the analyzing power angular distribution of outgoing ${}^3\text{He}$ and α particles. At high emission energy the analyzing power is characterized by generally large absolute values. This artifact is consistent with dominance of a direct interaction of the projectile with nucleons in the target. However, towards lower outgoing energy an increasing number of intranuclear N - N collisions preceding emission of the ejectile causes the analyzing power to be progressively quenched. Although only a limited number of target species have been explored, based on the nature of the reaction mechanism that is identified, this general feature is expected to be shared widely across the periodic target mass table.

Apart from the multistep part of the pre-equilibrium mechanism in $(\vec{p}, {}^3\text{He})$ reactions, the step which leads to emission of the composite ejectile is identified as pickup of two target nucleons in the final stage of the interaction. This can occur either as a first-step reaction process in which the projectile picks up a bound neutron-proton pair directly from the target, or in higher order steps as a pickup of two bound nucleons by any intranuclear projectile as the final stage after the statistical multistep N - N interactions [1–3].

The (\vec{p}, α) reaction also displays the same basic features expected for a statistical multistep component of the mechanism, but whether the final step involves pickup of three

nucleons or knockout of an α cluster seems to be somewhat controversial [4,5]. Investigations of exclusive (\vec{p}, α) reactions to discrete final excitations also suffer from this problem. For example, Gadioli *et al.* [9] show that cross section as well as analyzing power angular distributions of (\vec{p}, α) reactions on moderately heavy target masses can equally well be reproduced by distorted-wave Born approximation (DWBA) calculations which use pickup or knockout. On the other hand, Vergnes *et al.* [10] are confident, based on the study with unpolarized protons in a comparable mass and incident energy range, that the mechanism is triton pickup. Further confusion is introduced if we note that Bonetti *et al.* [11] conclude that in the case of $^{58}\text{Ni}(\vec{p}, \alpha)$ at an incident energy of 72 MeV, the transition to the ground state agrees only with a pickup mechanism, whereas the reaction into the continuum is undoubtedly a knockout mechanism. In fact, the inclusive reaction even has the wrong sign of the analyzing power for pickup.

In a recent study of $^{93}\text{Nb}(\vec{p}, \alpha)$ at incident energies between 65 and 160 MeV [5], we concluded that α -cluster knockout dominates at the lowest and possibly also at the highest projectile energies. However, at an incident energy of 100 MeV [5] both mechanisms seem to participate, with, if anything, pickup being more prominent. In this paper we present new results for ^{59}Co at an incident energy of 100 MeV, for which we found an even stronger indication of a contribution of both processes. We also now further investigate the seemingly erratic trend of the mechanism of the $^{93}\text{Nb}(\vec{p}, \alpha)$ reaction. This entails a simple consideration of how the two components of the mechanism react to the very large momentum mismatch between the incident and exit channels experienced in (\vec{p}, α) reactions. It is explained why this influences the energy-dependent yields of the two mechanisms differently. Consequently the variation of the relative cross sections from knockout and pickup as a function of projectile energy is judged to be reasonable.

Preliminary accounts of the results and ideas reported in this paper were presented at an international conference [12,13],

*aac@sun.ac.za

†sevdin@inrne.bas.bg

but now considerably more complete details and descriptions are provided.

In Sec. II the experimental procedure is described. A brief summary of the theoretical implementation is presented in Sec. III. Results are presented and discussed in Sec. IV. Finally, in Sec. V a summary is provided and conclusions are drawn.

II. EXPERIMENTAL PROCEDURE

The present data on $^{59}\text{Co}(\vec{p},\alpha)$ at an incident energy of 100 ± 0.5 MeV were measured at the cyclotron facility of iThemba Laboratory for Accelerator Based Sciences (LABS), Faure, South Africa during the same period as our previous experiment on ^{93}Nb . Details of the experimental technique were presented in Ref. [5], therefore only a brief description is provided here.

Two identical detector telescopes, collimated to a solid angle acceptance of about 1.1 msr, were positioned symmetrically with respect to the incident beam in a 1.5-m-diameter scattering chamber. Each telescope consisted of a 500- μm silicon surface-barrier detector followed by a NaI(Tl) crystal coupled to a phototube. Scattering angles were set to an accuracy of better than 0.2° with respect to the incident beam. The incident beam was polarized to a nominal values in a range of 70–80% perpendicular to the reaction plane. The direction of the polarization was switched at 5-s intervals during measurements. The choice of detector placement, together with the switching of the polarization direction, minimized systematic errors in the analyzing power measurements. Two metal targets (100% natural occurrence in the isotope ^{59}Co) had nominal thicknesses of 1 and 5 mg/cm², respectively. The uncertainty in these thicknesses was the main contribution of approximately 8% systematic error in the cross section scale. Of course, analyzing power, which consists of a ratio of cross sections, is not affected by this.

A ^{228}Th source was used for energy calibration of the Si detectors and the response of the NaI crystals was determined with proton scattering from a $(\text{CH})_n$ target. This procedure gives an overall accuracy of the emission-energy scale of better than 4%.

Cross sections and analyzing powers were binned in 4-MeV-wide intervals in the E_α emission-energy scale. The minimum α -particle energy E_α of 34 MeV, at which data were measured in this experiment, is very close to the stopping value as given by the nominal thickness of the Si detectors. Therefore special care was taken at this energy to make sure that data are not partially lost due to the lower limit of the detectors.

Standard electronics processed signals from the detectors and an online computer system was used for data accumulation. A ΔE - E energy-loss technique was employed for particle identification, and raw data were also stored online for later replay.

III. THEORETICAL ANALYSIS

We describe the (\vec{p},α) inclusive reactions at an incident energy of 100 MeV as a pre-equilibrium reaction. We assume that this type of reaction occurs in a series of intranuclear N - N scattering events followed by a final process in which the α

particle is emitted. The single step direct reaction can be a knockout of an α cluster or a pickup of a triton.

The theory applied to the (p,α) reaction is based on the multistep direct theory of Feshbach, Kerman, and Koonin (FKK) [7].

The double-differential cross section within the statistical multistep direct model [7] is a sum of terms related to one-, two- and further steps:

$$\frac{d^2\sigma}{d\Omega dE} = \left(\frac{d^2\sigma}{d\Omega dE} \right)^{1\text{-step}} + \left(\frac{d^2\sigma}{d\Omega dE} \right)^{2\text{-step}} + \dots, \quad (1)$$

The first-step cross section represents the direct transfer reaction, calculated in terms of the DWBA as

$$\left(\frac{d^2\sigma}{d\Omega dE} \right)^{1\text{-step}}_{(p,\alpha)} = \sum_{N,L,J} \frac{(2J+1)}{\Delta E} \frac{d\sigma^{\text{DW}}}{d\Omega}(\theta, N, L, J, E), \quad (2)$$

where the differential cross sections $d\sigma^{\text{DW}}/d\Omega$ to particular (N, L, J) states are calculated using the computational code DWUCK4 [14].

To calculate the distorted waves in the incident and the outgoing channels we use the hybrid nucleus-nucleus optical potential [15]. It has real and imaginary parts expressed as

$$U(\mathbf{r}) = N^R V^{DF}(\mathbf{r}) + i N^I W^{DF}(\mathbf{r}), \quad (3)$$

which generally depend on the radius-vector \mathbf{r} connecting centers of the interacting nuclei. The parameters N^R and N^I correct the strength of the microscopically calculated real V^{DF} and imaginary W^{DF} constituents of the whole potential.

In previous studies of the $^{93}\text{Nb}(\vec{p},\alpha)$ reaction [4,5,16] we selected the spin-orbit part of the optical potentials from phenomenological potentials available in the literature. However, in the present set of calculations, although we still use a standard form of the spin-orbit potential, the depth and the geometrical parameters of the derivative Woods-Saxon potential are derived from the double folding potential of Eq. (3). This procedure allows us to reduce the number of the phenomenological parameters and to construct all parts of the optical potentials in a consistent way. A description of the implementation of the folding model is provided in Refs. [4,5].

The scaling parameters of the double folding potentials N^R and N^I are determined by fitting the differential cross section and the analyzing power at the highest outgoing energy of $E_\alpha = 98$ MeV where only the first-step direct emission takes place. The values of the parameters which reproduce best the experimental data are $N^R = 0.5$ and $N^I = 0.08$ for the incident channel and $N^R = 1.0$ and $N^I = 1.0$ for the outgoing channel.

In our previous study of $^{93}\text{Nb}(\vec{p},\alpha)$ [5] the justification for using a folded optical potential instead of phenomenological parameters was discussed in terms of a desire to treat the incident and exit channels on equal footings. As indicated in Eq. (3), the folded optical potential has only two adjustable parameters N^R and N^I for renormalization of the microscopically calculated potentials. We speculate that renormalization could compensate for inadequacies in the resultant optical potentials.

For the incident channel $p + ^{93}\text{Nb}$ [5] no renormalization of the folded optical potential was needed, but now for $p + ^{59}\text{Co}$,

as was already mentioned, $N^R = 0.5$ and $N^I = 0.08$ are required for best reproduction of the experimental data. Of course, these latter values, especially the imaginary part, are seriously out of line with the earlier results. However, explicit calculations for ^{59}Co in which we use the same phenomenological spin-orbit optical potential as in our previous work on ^{93}Nb confirm that the new normalizations are purely an artifact of the current folding model based spin-orbit potential. A comparable treatment of the spin-orbit potential done earlier [5] gives consistent values of $N^R = N^I = 1$, with fairly similar agreement between the theoretical results and the experimental distributions as presented in this paper. Although this result is interesting, it is beyond the scope of the present work to explore this issue further.

When the emission energy decreases the multistep contributions to the calculated observables have to be taken into account. In terms of the FKK theory [7] the two-step cross section is calculated as a convolution of the (p, p') cross section and the direct (p, α) cross section:

$$\left(\frac{d^2\sigma}{d\Omega dE} \right)^{2\text{-step}} = \int \frac{d\mathbf{k}}{(2\pi)^3} \left(\frac{d^2\sigma(\mathbf{k}_i, \mathbf{k})}{d\Omega_i dE_i} \right)_{(p, p')} \left(\frac{d^2\sigma(\mathbf{k}, \mathbf{k}_f)}{d\Omega_f dE_f} \right)^{1\text{-step}}_{(p, \alpha)}, \quad (4)$$

where \mathbf{k}_i , \mathbf{k} , and \mathbf{k}_f are the momenta of the initial, the intermediate, and the final steps. Analogously we calculate the third-step double-differential cross section.

The theoretical (p, p') and (p, p', p'') double-differential cross section distributions which are needed to calculate the contributions of the second- and third-step processes were derived in Refs. [17, 18]. These cross section distributions were extracted by means of a FKK multistep direct reaction theory, which reproduce experimental inclusive (p, p') quantities [17] on target nuclei which are close to those needed for this work and are in an appropriate incident energy range. Interpolations and extrapolations in incident energy and target mass were introduced to match the specific requirements accurately.

To take into account the intermediate steps which involve neutrons, such as (p, n, α) , we assumed that different nucleons may be treated on an equal footing in the multistep part of the reaction. This meant that a simple renormalization of the (p, p') and (p, p', p'') cross sections could be introduced to correct for the influence of the intermediate counterparts which involve neutrons. In these present calculations we take into account explicitly the (p, n, α) process by assuming that $d^2\sigma^{(p, n)}/d\Omega dE = d^2\sigma^{(p, p')}/d\Omega dE$ and also the four possible combinations of two-step intranuclear collisions (p, x, x) , $x = n, p$, with $d^2\sigma^{(p, x, x)}/d\Omega dE = d^2\sigma^{(p, p', p'')}/d\Omega dE$.

The extension of the FKK theory from cross sections to analyzing power is described by Bonetti *et al.* [19]. The multistep expression for the analyzing power becomes

$$A_{\text{multistep}} = \frac{A_1 \left(\frac{d^2\sigma}{d\Omega dE} \right)^{1\text{-step}} + A_2 \left(\frac{d^2\sigma}{d\Omega dE} \right)^{2\text{-step}} + \dots}{\left(\frac{d^2\sigma}{d\Omega dE} \right)^{1\text{-step}} + \left(\frac{d^2\sigma}{d\Omega dE} \right)^{2\text{-step}} + \dots}, \quad (5)$$

with A_i , $\{i = 1, 2, \dots\}$ referring to analyzing powers for the successive multisteps.

As was already mentioned in the Introduction, we concluded that the reaction mechanism in the $^{93}\text{Nb}(\vec{p}, \alpha)$ reaction changes from a dominant knockout process at 65 MeV incident energy, to a combination of pickup and knockout participating at 100 MeV, and then back to only knockout being important at 160 MeV [5]. Now in the study of the $^{59}\text{Co}(\vec{p}, \alpha)$ reaction at 100 MeV we again consider the possibility of the presence of both reaction mechanisms. The scaling factors for the differential cross sections for each type of mechanism, as needed to fit the experimental differential cross sections at an emission energy of 98 MeV, are kept unchanged for the rest of the calculations at other outgoing energies.

IV. RESULTS AND DISCUSSION

A. Emission-energy angular distributions for ^{59}Co

Cross section and analyzing power angular distributions are shown for a selection of emission energies for the $^{59}\text{Co}(\vec{p}, \alpha)$ reaction at an incident energy of 100 MeV in Fig. 1. Theoretical calculations for pickup, knockout, and a combination of both mechanisms are compared with the experimental distributions.

As was found in previous (\vec{p}, α) and $(\vec{p}, {}^3\text{He})$ studies [1–5] the multistep character of the pre-equilibrium reaction is very noticeable as the emission energy drops towards lower values. For example, whereas the analyzing power displays large (negative) values at forward angles at the highest emission energy E_α , values get progressively weaker at lower outgoing energies. At $E_\alpha = 34$ MeV the analyzing power settles at essentially zero over the whole angular range. In our earlier work this trend was consistently shown to occur as a direct consequence of participation of an increasing number of intranuclear N - N steps as the emission energy drops.

As is noticeable in Fig. 1, there is only a very slight difference between the two sets of shapes of cross section and analyzing power angular distributions predicted for the two mechanisms considered, namely knockout or pickup, as the terminating step in the reaction chain. Consequently the results do not show a preference for one mechanism over the other. It is nevertheless interesting that even better agreement between the theoretical distributions and experimental data is obtained if a combination of knockout and pickup components, as shown in Fig. 1, is adopted. Cross section normalizations are arbitrarily adjusted for best agreement between the theoretical and experimental results. The normalization for each reaction type is kept constant for all emission energies, therefore the remaining variation in ratios are those which are inherent to each reaction type. In the present study of $^{59}\text{Co}(\vec{p}, \alpha)$ the two mechanisms appear to be roughly equally prominent, especially at the higher emission energies.

Although we previously [5] also concluded that a mixture of knockout and pickup gives the best results for $^{93}\text{Nb}(\vec{p}, \alpha)$ at the same projectile energy of 100 MeV, pickup nevertheless appeared to be the dominant process for the specific reaction on that target. However, for both lower (65 MeV [5]) and higher (160 MeV [4]) incident energies on ^{93}Nb , we concluded that the mechanism appears to require only knockout to account for the experimental analyzing power distributions. Although we have not studied ^{59}Co at higher and lower incident energies

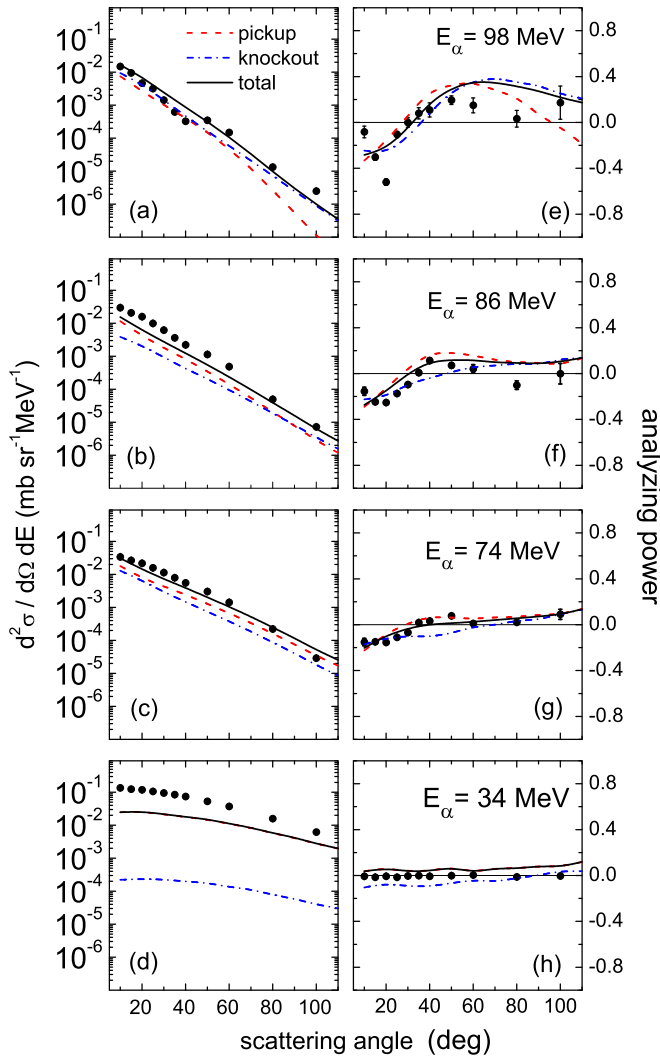


FIG. 1. Double-differential cross sections (a)–(d) and analyzing power (e)–(h) as a function of scattering angle for the $^{59}\text{Co}(\vec{p}, \alpha)$ reaction at an incident energy of 100 MeV and various α -particle emission energies E_α as indicated. Theoretical calculations of cross section and analyzing power distributions for pickup (---) and knockout (---), with the sums of both reaction mechanisms plotted as continuous curves, are compared with experimental quantities.

for comparison, it nevertheless becomes crucial to understand the validity of the incident-energy trend for the heavier target nucleus. We investigate this in detail in the next subsection.

B. Incident-energy behavior of the $^{93}\text{Nb}(\vec{p}, \alpha)$ reaction

The basic features of the $^{93}\text{Nb}(\vec{p}, \alpha)$ reaction at 65, 100, and 160 MeV have been presented earlier in Ref. [4,5], but now we provide additional insight which we discuss in detail.

As was already mentioned, at an incident energy of 65 MeV the $^{93}\text{Nb}(\vec{p}, \alpha)$ reaction appears to be best described as purely a knockout process convoluted in the basic multistep mechanism. As justification for this conclusion, analyzing power angular distributions are shown in Fig. 2 at an incident energy of 65 MeV. Theoretical predictions comprising either knockout or pickup are compared with experimental values.

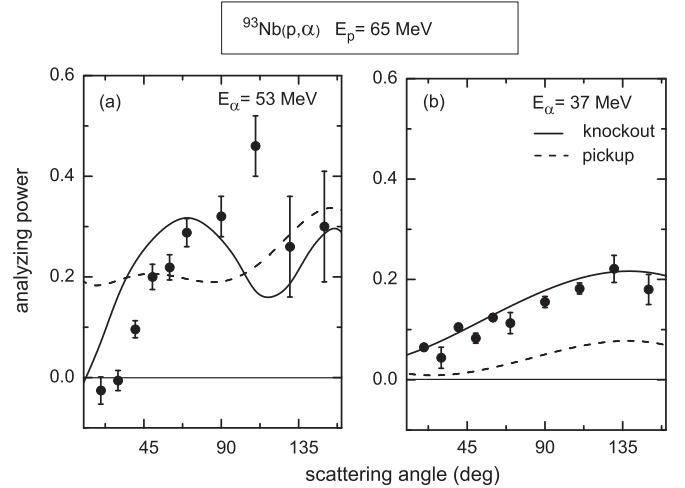


FIG. 2. Analyzing power (a)–(b) as a function of scattering angle for the $^{93}\text{Nb}(\vec{p}, \alpha)$ reaction at an incident energy of 65 MeV at emission energies E_α as indicated. Results for a knockout reaction mechanism are represented by continuous curves and those for a pickup mechanism are shown as dashed curves. Results are derived from those in Ref. [5].

These sets were chosen for illustration because high emission energy samples mostly the first, direct step, whereas higher order steps contribute at the low emission energy.

As shown in Fig. 2(a), experimental analyzing power values for $^{93}\text{Nb}(\vec{p}, \alpha)$ rise steeply from negative values to about 0.3 up to about 90° . This trend is matched reasonably well by knockout, but pickup values remain at a roughly constant value of 0.2 in this angular range. Such a prominent difference between the theoretical distributions is indicative of a very strong preference for a knockout mechanism.

In Fig. 2(b) knockout gives a good reproduction of the shape and magnitude of the analyzing power angular distribution. Although pickup also gives roughly the right shape, one should keep in mind that in terms of analyzing power a magnitude which is about a factor of 4 too small is unreasonably drastic.

As a further test we investigated a combination of pickup and knockout for this reaction at an incident energy of 65 MeV. As would be expected, any inclusion of the former reaction process only served to weaken the agreement drastically between theoretical prediction and experimental values, both for cross section and analyzing power.

In Fig. 3 analyzing power angular distributions for the reaction $^{93}\text{Nb}(\vec{p}, \alpha)$ at an incident energy of 100 MeV are shown. Again a high and a low emission energy are shown as typical examples. Now we find, in contrast to the situation at 65 MeV incident energy in Fig. 2, that the theoretical predictions for knockout and pickup both have very similar shapes as the experimental distributions at both emission energies. However, for knockout, the values are significantly higher than would be considered to be desirable. In fact at the lower emission energy the distribution is now consistently a factor of 4 too high for knockout. Given a choice between knockout and pickup, we are forced to favor the latter. If we again go through the exercise of finding a favorable mix between pickup and knockout, we now find that we can get

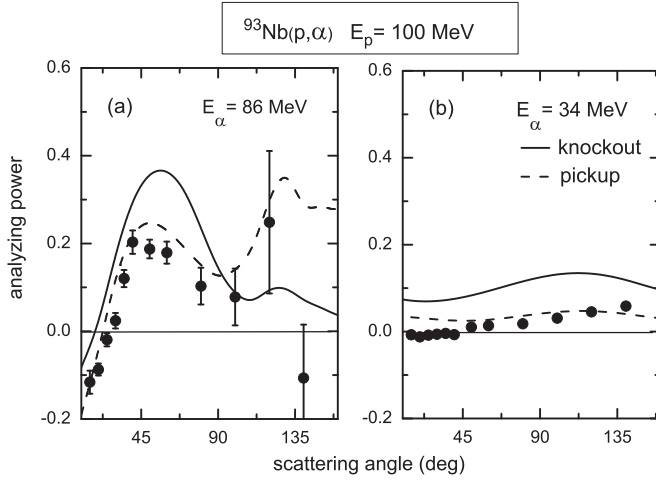


FIG. 3. Results for $^{93}\text{Nb}(\vec{p}, \alpha)$ as described in the caption to Fig. 2, but for an incident energy of 100 MeV. Results are derived from those in Ref. [5].

better agreement between theory and experimental data if we include some knockout. The result of this was presented in Ref. [5]. Note that pickup was still the dominant component at an incident energy of 100 MeV, which is in strong contrast with the conclusion reached at 65 MeV that there knockout is the main process.

Finally, for $^{93}\text{Nb}(\vec{p}, \alpha)$ at an incident energy of 160 MeV, as discussed in Ref. [4], a comparison similar to those presented in Figs. 2 and 3 was not really conclusive, although knockout appeared to be more likely. The justification for choosing knockout as the more likely process was discussed in [4].

Irrespective of whether the interpretation at the upper end of incident energy found in Ref. [4] is correct or not, the reaction mechanism for $^{93}\text{Nb}(\vec{p}, \alpha)$ thus seems to develop in an unusual way between 65 and 160 MeV. The likely contrasting way in which knockout and pickup mechanisms could behave may provide insight into the probable cause of the postulated behavior. At the very least it should be investigated whether such a behavior is even in principle possible. This is discussed in the next subsection.

C. Important kinematic constraints in knockout and pickup mechanisms for the $^{93}\text{Nb}(\vec{p}, \alpha)$ reaction

As was mentioned in Ref. [5], a (p, α) reaction has a very large momentum difference q between the incident and exit channels. This momentum difference grows with increasing incident energy. Also, as is well known, in a pickup reaction large angular-momentum transfer L would partially compensate for linear momentum mismatch q , and that is the reason why the cross section of a direct (p, α) pickup reaction for a specific L transfer is peaked at an incident energy for which the combination of L and q is favorable. Simplistically stated, large angular momentum transfer L is available due to pickup of valence nucleons with large orbital angular momentum ℓ . Angular momentum transfers which do not satisfy the requirement for minimum overall momentum mismatch in a pickup reaction clearly contribute less to the cross section.

Knockout, on the other hand, is perfectly momentum matched by means of three-body kinematics [20] only when the projectile and the struck α particle both emerge from the target system at so-called coplanar quasifree angles [21]. However, in a pre-equilibrium reaction it has to be taken into account that in any knockout process it is very likely that one of the emerging products would be absorbed in the residual target system. In the case of an α particle scattered to a forward angle, this will be the only candidate which is likely to escape. Consequently, for pre-equilibrium reactions, knockout kinematics is in practice subject to the same basic restriction as imposed by the momentum difference between incident and exit channels as for a pickup mechanism. However, whereas large L transfers are accessible to pickup, α clusters are likely to have only low angular momentum relative to the core. This follows from explicit knockout studies (see for example [22]), in which zero relative angular momentum for bound clusters dominates for even-even target nuclei. This means that, for knockout, momentum mismatch would not usually be minimized as a result of momentum transfer, as would be the case for pickup.

In the theoretical formalism of knockout and pickup, the distorted wave function $|\psi(q)|^2$ of the bound system that is involved in the reaction, expressed in momentum space q , is significant (see for example [20]). Cross sections σ are, amongst other ingredients, roughly proportional to $|\psi(q)|^2$. Consequently knockout cross sections, as encountered in inclusive reactions, should follow the trend of the wave function at large momentum mismatch, and those of pickup would follow the roughly Gaussian-shaped wave function [21,23] around a momentum-matched region.

In Fig. 4 these ideas, which strongly influence the incident-energy trend of cross section yields of knockout and pickup reactions, are explored in terms of explicit, albeit simplistic, DWBA calculations. The results are plotted as a function of overall momentum mismatch (with the scale of the incident energy also indicated) for relatively high emission energies (only 20 MeV lower than the incident energy) at a forward scattering angle where a direct single-step process dominates.

The momentum mismatch q_{match} , with α -particle emission in the same direction as the momentum of the incident projectile, is calculated as

$$q_{\text{match}} = q_{\alpha} - q_p - q_L, \quad (6)$$

where q_p and q_{α} are the momenta of the incident proton and outgoing α particle, respectively, and q_L is the momentum associated with the angular momentum transfer L . For pickup

$$q_L = \frac{\hbar L}{r_0 A^{1/3}} \approx 290 \text{ MeV}/c, \quad (7)$$

if values of $r_0 = 1.2$, core mass $A = 90$, and $L = 8$ are used. For knockout, as was discussed already, $L = 0$ (and $q_L = 0$).

At 65 MeV and 160 MeV incident energies, the experimental cross sections for the alternative pickup process are arbitrarily assigned to be 10% of those resulting from the main knockout process, as extracted in Refs. [4,5]. This value follows because such a pickup contribution would be interpreted as being below the level of observation in the context of the accuracy of identification of the reaction

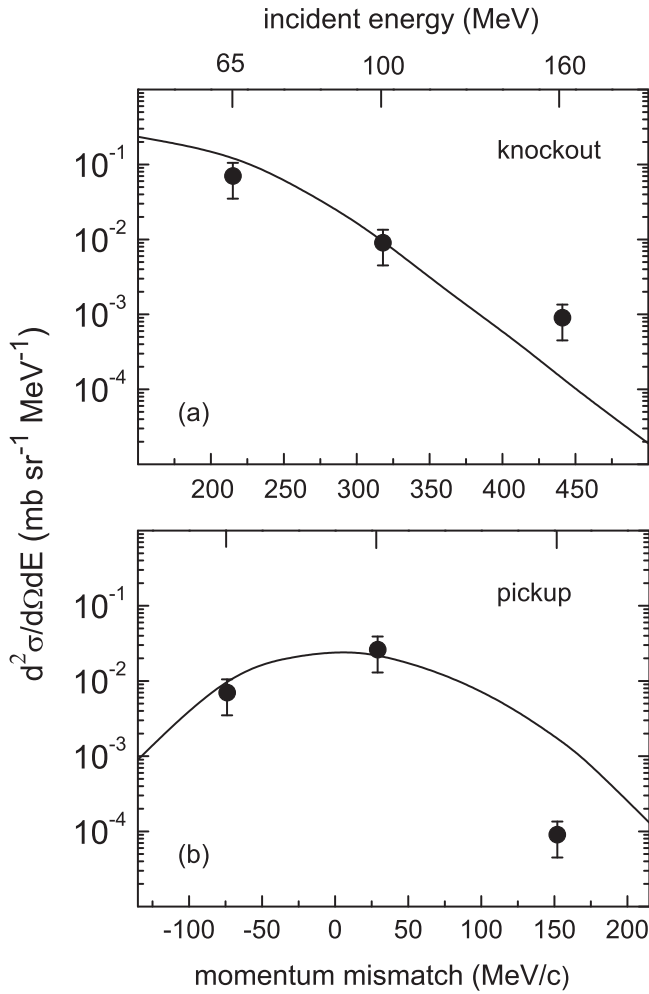


FIG. 4. Double-differential cross section for the $^{93}\text{Nb}(\bar{p},\alpha)$ reaction corresponding to yields from a knockout mechanism (a) and pickup (b). Results at emission energies 20 MeV lower than the incident energies are shown as a function of momentum mismatch (scales on the lower horizontal axes) and the incident energy for both panels is indicated on the top horizontal axis of (a). The curves are DWBA predictions as described in the text.

mechanism. Of course, a proportion of anything from 0–20% would qualify as negligible pickup at the lowest and highest incident energies. At an incident energy of 100 MeV, where both mechanisms are clearly identifiable, the ratio used is the one found [5] to fit the combined statistical multistep theoretical results to the experimental cross sections.

An angular momentum transfer of $L = 8$ represents the optimum matching condition as implied by the resultant momentum scale for pickup in Fig. 4(b), which results in a distribution more or less centered around zero momentum mismatch. Of course, other angular-momentum values may also participate in a pickup reaction, but, as implied earlier, the main contribution to the cross section yield comes from the L value which minimizes the momentum mismatch. Such an approximation of a single optimum angular momentum transfer is known to be reasonable [24], and its validity is understood for the two-nucleon pickup reaction $^{58}\text{Ni}(p, {}^3\text{He})^{56}\text{Co}$

to discrete final states at incident energies between 80 and 120 MeV. It follows that the same principle should apply to the $^{93}\text{Nb}(\bar{p},\alpha)$ reaction into the continuum of final energies.

For comparison with the experimental knockout component, DWBA cross sections are shown in Fig. 4(a) as a function of momentum mismatch without any adjustment from angular momentum transfer available. This is consistent with our assumption of either zero or small relative angular momentum of the knocked-out cluster relative to the core in the target nucleus.

Although the folding potentials as described in Sec. III could have been used for the DWBA calculations in Fig. 4, for convenience these predictions of the incident-energy dependence of the pickup cross sections were performed with potentials for protons from Ref. [25] and α particles from Ref. [26]. The specific choice of optical potentials and bound-state geometry mainly affects the overall (unknown) absolute cross section, but because this may be arbitrarily renormalized to reproduce the experimental yields, this is of no consequence here.

Clearly the basic increase of the experimental pickup yield from 65 to 100 MeV in Fig. 4(b), with a subsequent drop towards 160 MeV, is reproduced well by the theory. The almost exponential drop with increasing momentum mismatch as found experimentally for knockout in Fig. 4(a) is also reproduced accurately with the DWBA calculations. Of course, for a quantitative appreciation of the observed relative magnitudes of knockout and pickup we need additional information, such as spectroscopic factors and α -cluster preformation probabilities. In the absence of proper guidance, normalizations between theoretical results and experimental as found are not unacceptable.

As was mentioned in Sec. IV A, the reaction $^{59}\text{Co}(\bar{p},\alpha)$ at an incident energy of 100 MeV follows a similar mix of pickup and knockout as $^{93}\text{Nb}(\bar{p},\alpha)$ at the same projectile energy. It would be of interest to explore the reaction mechanism for ^{59}Co at both lower and higher incident energies, for which ^{93}Nb shows a strong preference for the knockout mechanism. It is already known that at 72 MeV incident energy for the reaction $^{58}\text{Ni}(\bar{p},\alpha)$, which is close in target mass to ^{59}Co , a previous study [11] indicates overwhelming dominance of knockout. Also, at higher incident energies up to 200 MeV [18], knockout appears to describe experimental cross section distributions of unpolarized $^{59}\text{Co}(p,\alpha)$ well. Consequently it would not be surprising if ^{59}Co and ^{93}Nb follow the same trend in the ratio of knockout and pickup with incident energy.

V. SUMMARY AND CONCLUSIONS

New experimental data for the reaction $^{59}\text{Co}(\bar{p},\alpha)$ at an incident energy of 100 MeV into the continuum of excitation were presented. The cross section and analyzing power angular distributions at a large range of emission energies are reproduced well by a statistical multistep pre-equilibrium theory, in which a combination of terminating knockout and pickup processes are major ingredients. The mix of mechanisms extracted from the theoretical analysis is qualitatively similar to results previously found at the same incident energy for the target nucleus ^{93}Nb .

The energy-dependent trend of the mechanism previously found for $^{93}\text{Nb}(\vec{p}, \alpha)$ between 65 and 160 MeV was studied more carefully in this work. Because of the substantial difference, especially at these incident energies, between the momenta of the projectile and outgoing α particle in (p, α) reactions, large values of angular momentum transfer L are required to eliminate momentum mismatch. It is argued that pickup involves an appropriate range of angular momentum transfers, whereas a knockout process is restricted to low L . This difference should have a far-reaching consequence for the cross section trends as a function of incident energy for the two competing reaction mechanisms. The validity of these ideas was explored with simplistic DWBA calculations in an excitation-energy range where a single-step reaction mechanism should be important. Only a single appropriate L value was employed as a reasonable approximation of the pickup trend. The predicted variation of the cross section with incident energy proved to be in fairly good agreement with the experimental distribution.

Participation of preformed α clusters with $L = 0$ was assumed for the knockout part of the reaction. Also for this mechanism the simplistic DWBA calculation provided a good reproduction of the experimental measurements.

The results of the simple DWBA calculations substantiate the conclusions drawn from the more elaborate and complete

statistical multistep theoretical approach. The present work implies that the incident energy trend of the $^{59}\text{Co}(\vec{p}, \alpha)$ reaction would be driven by the same considerations as those of $^{93}\text{Nb}(\vec{p}, \alpha)$, with only inconsequential detail variations as a result of nuclear structure differences. Clearly it would be useful to extend the present work to ^{59}Co at both lower and higher incident energies to confirm the expectation.

Properties of momentum distributions of preformed α clusters in odd nuclei are largely unknown, and for this work we were therefore forced to extrapolate from knowledge regarding even-even nuclides. Further quasifree α -cluster knockout studies to clarify these issues would be invaluable.

ACKNOWLEDGMENTS

Our appreciation is extended to G. F. Steyn and S. V. Förtsch for providing the numerical data at an incident energy of 100 MeV reported in this work. The research of A.A.C. was funded by the National Research Foundation (NRF) of South Africa Grant No. 80833. The studies of S.S.D. were partially supported by the DFNI-T02/19 grant of the Bulgarian Science Foundation. E.V.Z. and K.V.L. were supported by the Russian Foundation for Basic Research (RFBR) under Grant No. 13-01-00060a. This financial support is gratefully acknowledged.

-
- [1] A. A. Cowley, G. F. Steyn, S. S. Dimitrova, P. E. Hodgson, G. J. Arendse, S. V. Förtsch, G. C. Hillhouse, J. J. Lawrie, R. Neveling, W. A. Richter, J. A. Stander, and S. M. Wyngaardt, *Phys. Rev. C* **62**, 064605 (2000).
 - [2] A. A. Cowley, J. Bezuidenhout, S. S. Dimitrova, P. E. Hodgson, S. V. Förtsch, G. C. Hillhouse, N. M. Jacobs, R. Neveling, F. D. Smit, J. A. Stander, G. F. Steyn, and J. J. van Zyl, *Phys. Rev. C* **75**, 054617 (2007).
 - [3] A. A. Cowley, J. J. van Zyl, S. S. Dimitrova, E. V. Zemlyanaya, and K. V. Lukyanov, *Phys. Rev. C* **85**, 054622 (2012).
 - [4] S. S. Dimitrova, A. A. Cowley, J. J. van Zyl, E. V. Zemlyanaya, and K. V. Lukyanov, *Phys. Rev. C* **89**, 034616 (2014).
 - [5] S. S. Dimitrova, A. A. Cowley, E. V. Zemlyanaya, and K. V. Lukyanov, *Phys. Rev. C* **90**, 054604 (2014).
 - [6] E. Gadioli and P. E. Hodgson, *Pre-Equilibrium Nuclear Reactions* (Oxford University Press, New York, 1991).
 - [7] H. Feshbach, A. Kerman, and S. Koonin, *Ann. Phys. (N.Y.)* **125**, 429 (1980).
 - [8] A. J. Koning and J. M. Akkermans, *Phys. Rev. C* **47**, 724 (1993).
 - [9] E. Gadioli, E. Gadioli-Erba, P. Guazzoni, P. E. Hodgson, and L. Zetta, *Z. Phys. A* **318**, 147 (1984).
 - [10] M. Vergnes, G. Rotbard, J. Kalifa, and G. Berrier-Ronsin, *Phys. Rev. C* **10**, 1156 (1974).
 - [11] R. Bonetti, F. Crespi, and K.-I. Kubo, *Nucl. Phys. A* **499**, 381 (1989).
 - [12] A. A. Cowley, S. S. Dimitrova, E. V. Zemlyanaya, K. V. Lukyanov, and J. J. van Zyl, *EPJ Web Conf.* **107**, 08004 (2016).
 - [13] S. S. Dimitrova, A. A. Cowley, E. V. Zemlyanaya, and K. V. Lukyanov, *EPJ Web Conf.* **107**, 08005 (2016).
 - [14] P. D. Kunz and E. Rost, in *Computational Nuclear Physics*, edited by K. Langanke *et al.* (Springer-Verlag, Berlin, 1993), Vol. 2, Chap. 5.
 - [15] V. K. Lukyanov, E. V. Zemlyanaya, and K. V. Lukyanov, JINR preprint P4-2004-115, Dubna, 2004; *Phys. At. Nucl.* **69**, 240 (2006).
 - [16] S. S. Dimitrova and A. A. Cowley, in *Nuclear Theory: Proc. 33rd International Workshop on Nuclear Theory Rila, Bulgaria, June 22–28, 2014*, edited by A. Georgieva and N. Minkov (Heron Press, Sofia, 2014), p. 106.
 - [17] W. A. Richter, A. A. Cowley, G. C. Hillhouse, J. A. Stander, J. W. Koen, S. W. Steyn, R. Lindsay, R. E. Julies, J. J. Lawrie, J. V. Pilcher, and P. E. Hodgson, *Phys. Rev. C* **49**, 1001 (1994).
 - [18] A. A. Cowley, G. J. Arendse, J. W. Koen, W. A. Richter, J. A. Stander, G. F. Steyn, P. Demetriou, P. E. Hodgson, and Y. Watanabe, *Phys. Rev. C* **54**, 778 (1996).
 - [19] R. Bonetti, L. Colli Milazzo, I. Doda, and P. E. Hodgson, *Phys. Rev. C* **26**, 2417 (1982).
 - [20] N. S. Chant and P. G. Roos, *Phys. Rev. C* **15**, 57 (1977).
 - [21] P. G. Roos, N. S. Chant, A. A. Cowley, D. A. Goldberg, H. D. Holmgren, and R. Woody, *Phys. Rev. C* **15**, 69 (1977).
 - [22] T. A. Carey, P. G. Roos, N. S. Chant, A. Nadasen, and H. L. Chen, *Phys. Rev. C* **29**, 1273 (1984).
 - [23] A. N. Antonov, E. N. Nikolaev, I. Zh. Petkov, P. E. Hodgson, and G. A. Lalazissis, *Bulg. J. Phys.* **19**, 11 (1992).
 - [24] J. J. van Zyl, A. A. Cowley, R. Neveling, E. Z. Buthelezi, S. V. Förtsch, J. Mabiala, J. P. Mira, F. Nemulodi, F. D. Smit, G. F. Steyn, J. A. Swartz, and I. T. Usman, *Phys. Rev. C* **91**, 024614 (2015).
 - [25] A. J. Koning and J. P. Delaroche, *Nucl. Phys. A* **713**, 231 (2003).
 - [26] V. Avrigeanu, P. E. Hodgson, and M. Avrigeanu, *Phys. Rev. C* **49**, 2136 (1994).